Supporting Information

Dynamics of the ^{3}MLCT in Ru(II) Terpyridyl Complexes Probed by Ultrafast Spectroscopy: Evidence of Excited-State Equilibration and Interligand Electron Transfer

Joshua T. Hewitt, Paul J. Vallett, and Niels H. Damrauer*

Department of Chemistry and Biochemistry, University of Colorado, Boulder, Colorado 80309

Additional Information Regarding the Ultrafast Spectrometer:

Both the instrument response function (IRF) and temporal resolution of the spectrometer were characterized by cross-correlation of the pump and probe pulses in neat solvent. The IRF was quantified by fitting the envelop of the pump probe cross-correlation in neat acetonitrile to a Gaussian function.[1] Representative temporal FWHM value measured at 380, 400, 480, and 620 nm are 300 ± 24 fs, 280 ± 30 fs, 190 ± 25 fs and 210 ± 23 fs respectively. The error bars are based on several independent measurements. The measured IRF is much longer than the pump pulse duration as a result of significant chirp in our probe pulse and the relative thickness of our sample cell (1.25 mm windows and 2 mm sample volume; NGS Precision Cells, 61UV2). Because of the short excitation pulse, we are still able to resolve sub-50 fs dynamics as evidenced by the TA signal collected in neat chloroform shown in Figure S1.[2] Chirp correction in the kinetics and spectral data was accomplished by setting the positive peak of the pump-probe cross correlation signal to t = 0 for data collected at each respective wavelength.[1]

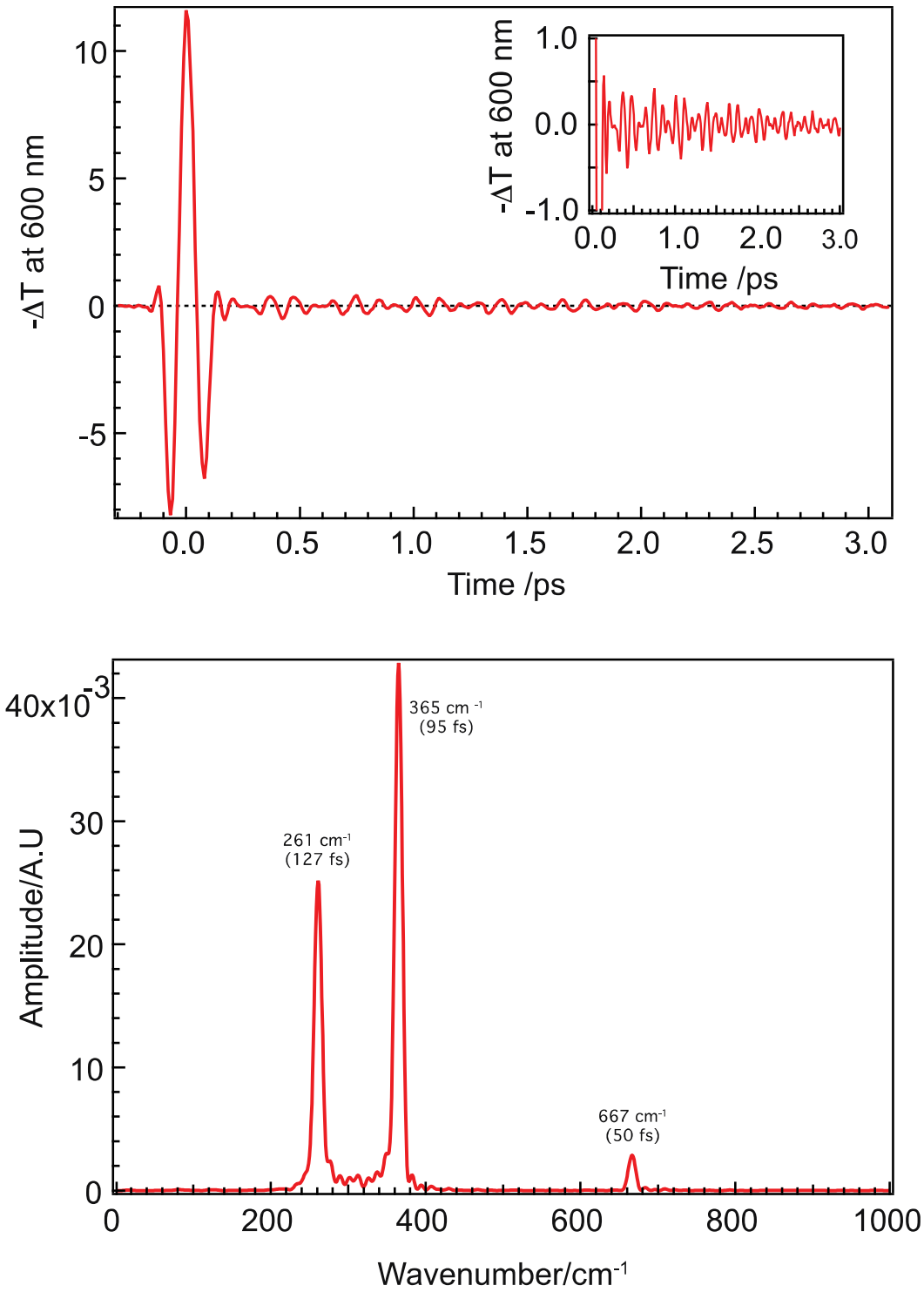

Figure S1. *Top:* Magic angle TA of neat $CHCl_3$ collected using a pump pulse centered at 525 nm and probing at 600 nm. The inset shows an enlarged picture of the observed beat pattern. *Bottom*: FFT of the data presented in the inset. The peaks at 260 cm^{-1} (period = 127 fs), 366 cm^{-1} (period = 91 fs), and 667 cm^{-1} (period = 50 fs) all correspond to known modes of $CHCl_3$.

Details of the Data Collection Procedures, Chirp Correction, and Fitting Practices Used for the Transient Data:

In calculating time points to visit in the single wavelength transient kinetics scans presented in the manuscript, the quasi-logarithmic approach to time step spacing of Riedle and co-workers[2] was employed. This approach ensures that the time decades from -1 to 1 ps, 1 to 10 ps, 10 to 100 ps… all contain an equal number of data points. Therefore, when fitting routines are applied to the data each temporal decade receives equally weight.

Global fitting of the data relied on functionality built into IGOR Pro and consisted of simultaneously fitting three spectrally distinct sets of kinetics data to an exponential model:

$$-\Delta T(t) = \Sigma_i \, A_i e^{-\frac{t}{tau_i}} + y_0 \qquad \text{Eq. S1}$$

Here, -ΔT(t) refers to the negative change in transmittance as a function of time (t), which is the way the data were collected and presented, and y_0 is a time independent offset. For $[Ru(tpy)(ttpy)_2]^{2+}$ and $[Ru(ttpy)_2]^{2+}$, single wavelength kinetics were collected at 400, 480, and 620 nm while for $[Ru(tpy)_2]^{2+}$ kinetics were collected at 380, 475 and 620 nm. The time constants and pre-exponential values reported in the manuscript are an average of the results from global fitting three independent data sets. Thus, a total of nine independent data traces, three per wavelength, were collected for each complex. The uncertainties reported (2σ) for data at any given wavelength are two times the standard deviation of the three independent data sets collected. To exclude artifacts of the pump-probe overlap in the fitting routine, only data points greater than ~ 400 fs after t = 0 were included. For the data collected at 380 nm, where the IRF is significantly longer, only data points greater than ~ 500 fs after t = 0 were included. Normalization of the raw -ΔT data was done by setting the value of the first data point used for fitting to 1 or -1 for absorptive or bleach signals respectively. The kinetics and spectra presented

in the manuscript represent an average of 4 scans.

Preliminary Transient Data for $[Ru(tpy)_2]^{2+}$ collected in Neat Water

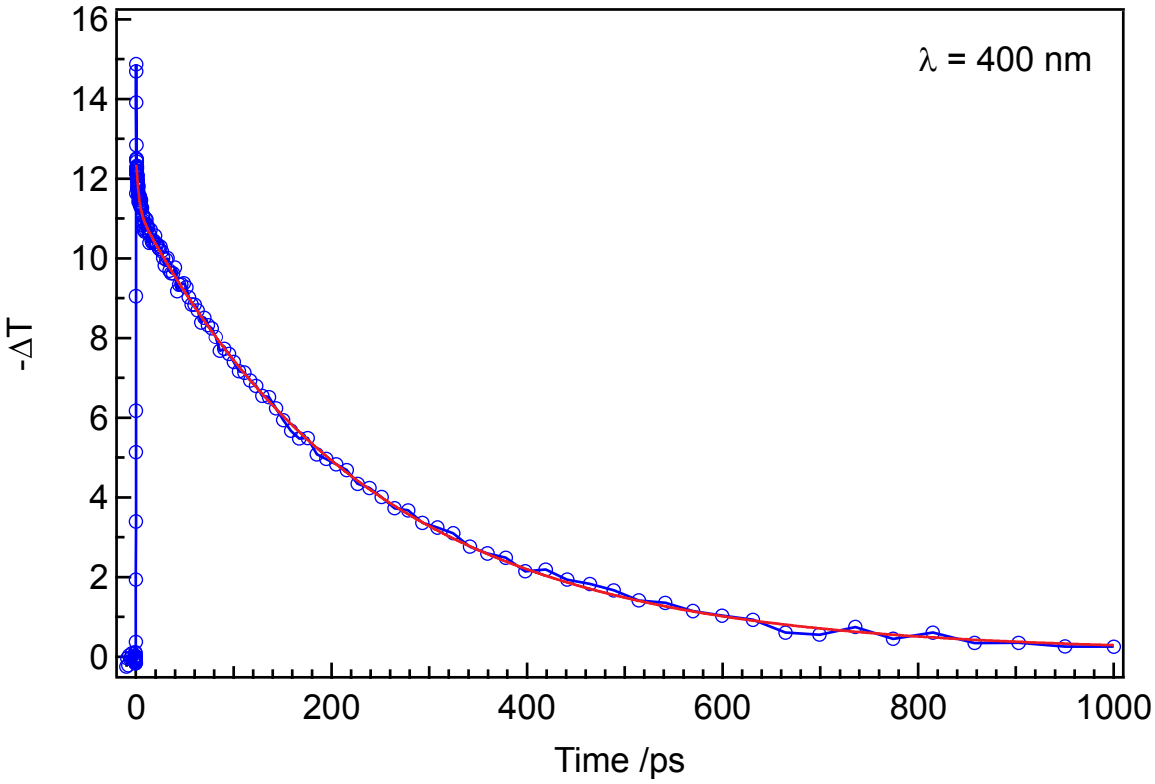

Figure S2. Kinetics of $[Ru(tpy)_2]^{2+}$ (excitation at 525 nm, probing at 400 nm) collected in room temperature water (blue) with a bi-exponential fit to the data in red. The recovered taus are ~ 2.6 and 238 ps respectively.

Deriving the ^{3}MLCT–^{3}MC K_{eq} and associated rate constants in $[Ru(tpy)_2]^{2+}$ using a pre-equilibrium assumption.

For clarity, we first restate Eq.1 from the manuscript below as Eq. S2:

$$^3\text{MLCT} \underset{k_b}{\overset{k_a}{\rightleftharpoons}} {}^3\text{MC} \xrightarrow{k_c} {}^1\text{GS} \qquad \text{Eq. S2}$$

Making use of a pre-equilibrium (between the ^{3}MLCT and ^{3}MC states) approximation, the equilibration timescale (referred to as τ_{Eq}, Eq. S3) and the long-time behavior of population in each state (Equations S4-6) can be expressed as follows:[3]

$$\tau_{Eq} = \frac{1}{k_a + k_b} \qquad \text{Eq. S3}$$

$$[MLCT](t) = \frac{k_b}{k_a + k_b}[MLCT_0]e^{-kt} \qquad \text{Eq. S4}$$

$$[MC](t) = \frac{k_a}{k_a + k_b}[MLCT_0]e^{-kt} \qquad \text{Eq. S5}$$

$$[GS](t) = [MLCT_0](1 - e^{-kt}) \qquad \text{Eq. S6}$$

$$\text{where, } k = \frac{k_a k_c}{k_a + k_b} \qquad \text{Eq. S7}$$

The 2.3 ps dynamics observed in the data collected at 380 and 620 nm is a direct measurement of τ_{Eq} while the overall 124 ps decay component is equal to *k*. If one assumes that ^{3}MLCT–^{3}MC equilibration is complete before any excited-state population is lost, the equilibrium amounts of ^{3}MLCT and ^{3}MC species, respectively, are given by:

$$[MLCT]_{Eq} = \frac{k_b}{k_a + k_b}[MLCT]_0 = k_b \times \tau_{Eq} \times [MLCT]_0 \qquad \text{Eq. S8}$$

$$[MC]_{Eq} = \frac{k_a}{k_a + k_b}[MLCT]_0 = k_a \times \tau_{Eq} \times [MLCT]_0 \qquad \text{Eq. S9}$$

Utilizing the measured equilibration time of 2.3 ps, the sum of the two preexponential components measured at 380 nm (1.08; which we assume directly reflects the initial ^{3}MLCT

population $[MLCT]_0$), and the preexponential of the long time component measured at 380 nm (0.92; reflecting $[MLCT]_{Eq}$), we can estimate $k_b = 0.37$ ps^{-1} directly from Eq. S8. With this value (and the equilibration time of 2.3 ps) we can determine $k_a = 0.064$ ps^{-1} from Eq. S3. The equilibrium constant $K_{eq} = 0.17$ follows from the expression $K_{eq} = k_a/k_b$. Finally, from the expression for k (Eq. S7) and its measure (1/124 ps), we can determine $k_c = 0.054$ ps^{-1} which is a measure of the ^{3}MC $\rightarrow$ ^{1}GS intersystem crossing rate constant.

Estimating the molar absorptivity of $[Ru^{III}(tpy^{\bullet-})(ttpy)]^{2+}$ and $[Ru^{III}(tpy)(ttpy^{\bullet-})]^{2+}$ species at 400 nm

To develop a deeper understanding of the spectro-temporal dynamics of $[Ru(tpy)(ttpy)]^{2+}$ following ^{1}MLCT excitation, we devised an analysis scheme to estimate the excited-state molar absorptivity of the tpy-localized ($[Ru^{III}(tpy^{\bullet-})(ttpy)]^{2+}$) and ttpy-localized ($[Ru^{III}(tpy)(ttpy^{\bullet-})]^{2+}$) species at 400 nm. At the outset it should be noted that measuring the absolute excited-state molar absorptivity of a complex using TA methods is difficult and requires, amongst other things, a detailed knowledge of the number of excited molecules in the sample, a homogenous transverse distribution of excited-states within the sample volume, and minimal amounts of scattering, fluorescence and phosphorescence.[4] Accordingly, the values reported herein are meant for comparative purposes only and should not be regarded as an accurate measurement of the true excited-state molar absorptivity of these complexes.

The transient signal at 400 nm in each complex is assumed to be composed of both excited-state absorption and ground state bleaching contributions. Therefore, the measured $-\Delta T/T$ signal can be approximated by Eq. S10 where ε_{ex} and ε_{gs} are the molar absorptivity of the

ground and excited-states at 400 nm, respectively, ℓ is the excitation path length, and N_{ex} is the number of excited-states.

$$-\frac{\Delta T}{T} \approx \left(\varepsilon_{ex} - \varepsilon_{gs}\right) * (\ell) * (N_{ex}) \qquad \text{Eq. S10}$$

This expression ignores emission, which occurs at much redder wavelengths in these complexes, as well as scattering. A homogenous distribution of excited-states within the sample volume is also assumed. Using the transient spectra collected at 10 ps (Figure F5), the values for ε_{gs} from our ground state molar absorption measurements, and the power and central frequency of the excitation laser pulse (needed to approximate the number excited-states), the ε_{ex} of $[Ru(tpy)_2]^{2+}$, $[Ru(tpy)(ttpy)]^{2+}$, and $[Ru(ttpy)_2]^{2+}$ at 400 nm are estimated to be 8,700 M^{-1} cm^{-1}, 13,200 M^{-1} cm^{-1}, and 22,200 M^{-1} cm^{-1}, respectively. For $[Ru(tpy)_2]^{2+}$, the value of 8,700 M^{-1} cm^{-1} in the ^{3}MLCT absorption is thought to be primarily due to reduced tpy ligand absorption while the value of 13,200 M^{-1} cm^{-1} for $[Ru(tpy)(ttpy)]^{2+}$ is attributed to the reduced ttpy ligand ($[Ru^{III}(tpy)(ttpy^{\bullet-})]^{2+}$). The value of 22,200 M^{-1} cm^{-1} in the ^{3}MLCT absorption of $[Ru(ttpy)_2]^{2+}$ is thought to be composed of both reduced *and* neutral ttpy ligand absorption. Therefore, using the value of 13,200 M^{-1} cm^{-1} for reduced ttpy ligand absorption, we estimate the neutral ttpy ligand molar absorptivity at 400 nm to be 9,000 M^{-1} cm^{-1}. With these values we can now estimate the molar absorption at 400 nm for the tpy-localized ($[Ru^{III}(tpy^{\bullet-})(ttpy)]^{2+}$) and ttpy-localized ($[Ru^{III}(tpy)(ttpy^{\bullet-})]^{2+}$) ^{3}MLCT configurations of $[Ru(tpy)(ttpy)]^{2+}$. For the tpy-localized configuration, absorption would result from both reduced tpy ligand *and* neutral ttpy ligand resulting in a total excited-state molar absorption of ~ 17,800 M^{-1} cm^{-1}. The ttpy-localized configuration would be primarily reduced ttpy ligand absorption resulting a total ^{3}MLCT molar absorption of only ~ 13,200 M^{-1} cm^{-1}. Therefore, the tpy-localized ^{3}MLCT is expected to be significantly more absorptive at 400 nm than the ttpy-localized ^{3}MLCT. Accordingly, as we

predict that the intial ^{3}MLCT has a significant amount of both tpy-localized and ttpy-localized ^{3}MLCT configurations, the overall absorptive signal at 400 nm can be expected to *decrease* as the system thermalizes to the low energy ttpy-configuration via ILET of the type $[Ru^{III}(tpy^{\bullet-})(ttpy)]^{2+} \rightarrow [Ru^{III}(tpy)(ttpy^{\bullet-})]^{2+}$. That this decrease in absorption is experimentally observed to be concomitant with an increase in the reduced ttpy absorption feature from 515 – 650 nm supports our assignment of the 3.3 ps dynamic to $[Ru^{III}(tpy^{\bullet-})(ttpy)]^{2+} \rightarrow [Ru^{III}(tpy)(ttpy^{\bullet-})]^{2+}$ ILET.

Complete citation for reference 86 in the manuscript:

Siemeling, U.; der Bruggen, J. V.; Vorfeld, U.; Neumann, B.; Stammler, A.; Stammler, H. G.; Brockhinke, A.; Plessow, R.; Zanello, P.; Laschi, F.; de Biani, F. F.; Fontani, M.; Steenken, S.; Stapper, M.; Gurzadyan, G. *Chem.-Eur. J.* **2003**, *9*, 2819-2833.

References

(1) Kovalenko, S. A.; Dobryakov, A. L.; Ruthmann, J.; Ernsting, N. P. *Phys. Rev. A* **1999**, *59*, 2369-2384.
(2) Megerle, U.; Pugliesi, I.; Schriever, C.; Sailer, C. F.; Riedle, E. *Appl. Phys. B* **2009**, *96*, 215-231.
(3) Rae, M.; Berberan-Santos, M. N. *J. Chem. Educ.* **2004**, *81*, 436-440.
(4) Bonneau, R.; Carmichael, I.; Hug, G. L. *Pure Appl. Chem.* **1991**, *63*, 290-299.